Analytical and Bioanalytical Chemistry (2023) 415:1305–1311
https://doi.org/10.1007/s00216-022-04419-3

RESEARCH PAPER

Peptide-anchored biomimetic interface for electrochemical detection of cardiomyocyte-derived extracellular vesicles

Yang Zhou[1] · Fei Zhao[1] · Bo Zheng[1] · Shihai Tang[1] · Juan Gong[1] · Bin He[1] · Zhi Zhang[1] · Na Jiang[1] · Huijuan Zha[1] · Jun Luo[1]

Received: 1 September 2022 / Revised: 20 October 2022 / Accepted: 31 October 2022 / Published online: 12 November 2022

Abstract

Cardiomyocyte-derived extracellular vesicles (EVs) are a promising class of biomarkers that can advance the diagnosis of many kinds of cardiovascular diseases. Herein, we develop a new electrochemical method for the feasible detection of cardiomyocyte-derived EVs in biological fluids. The core design of the method is the fabrication of a peptide-anchored biomimetic interface consisting of a lipid bilayer and peptide probes. On the one hand, the lipid bilayer provides excellent antifouling ability to the electrode interface and facilitates the anchoring of peptide probes. On the other hand, the peptide probes equip the electrode interface with excellent binding capability and affinity to CD172a, a specific marker of cardiomyocyte-derived EVs, thus enabling the efficient and selective detection of target EVs. Taking EVs derived from the heart myoblast cells H9C2 as the model target, the method displays a wide linear detection range from 1×10^3 to 1×10^8 particles/mL with a desirable detection limit of 132 particles/mL. Furthermore, the method shows good performance in biological fluids such as serum, and thus may have great potential for practical use in the diagnosis of cardiovascular diseases.

Keywords Lipid bilayer · Peptide probe · CD172a · Extracellular vesicle · Electrochemical detection

Introduction

Cardiovascular diseases, including but not limited to ischemic heart disease, heart failure, and stroke, are the leading cause of death worldwide [1]. Timely diagnosis is of great significance for effective treatment of patients with cardiovascular diseases, which may effectively shorten the length of hospital stay and reduce the mortality. Over the last decade, extracellular vesicles (EVs) derived from cardiomyocytes, especially small EVs (sEVs, also known as exosomes) with the diameter below 200 nm, have been found to be widely involved in the cardiac physiology and the progression of cardiovascular diseases [2, 3]. Moreover, emerging evidences suggest the potential role of cardiomyocyte-derived EVs in biological fluids as biomarkers to promote the diagnosis of cardiovascular diseases [4–6].

In the past few years, impressive progresses have been made on the development of detection methods for EVs with the increasing application of various analytical techniques [7–10]. Among them, electrochemical techniques have attracted considerable interest due to their high sensitivity, simplicity, and ease of integration with downstream electronic systems, which would facilitate the point-of-care diagnosis of diseases [11, 12]. Although some of electrochemical detection methods are proven to be clinically effective, they still face some obstacles when used to detect EVs of myocardial origin in biological fluids. On the one hand, components in biological fluids, such as proteins and cell debris, are easily adsorbed to the electrode interface in a non-specific manner, which may hinder the specific molecular recognition process and lead to false-negative results. On the other hand, EVs in biological fluids come from a wide range of sources, including not only EVs from cardiomyocytes but also a large number of EVs from other cells, which poses a high challenge to the selectivity of the detection method.

To address these shortcomings, we herein design a new electrochemical method for EVs detection based on

Published in the topical collection *Advances in Extracellular Vesicle Analysis* with guest editors Lucile Alexandre, Jiashu Sun, Myriam Taverna, and Wenwan Zhong.

✉ Yang Zhou
ZHA19940314@163.com

[1] Department of Cardiothoracic Surgery, People's Hospital of Leshan, Leshan, Sichuan 614000, People's Republic of China

a peptide-anchored biomimetic interface. The interface is prepared by the formation of a lipid bilayer on the electrode surface and the subsequent anchoring of peptide probes specific targeting to CD172a [13]. The lipid bilayer effectively reduces the non-specific adsorption of proteins and other components in biological fluids [14–17], thus improving the clinical usability of the method. At the meanwhile, the lipid bilayer stably interacts with the palmitoyl group modified at the end of peptide probes [18, 19], so that the probes can be anchored to the electrode surface in a facile way. Furthermore, peptide probes exhibit desirable capability and specificity in recognizing target biomolecules [20], thus ensuring the selective enrichment of CD172a-positive EVs, the typical cardiomyocyte-derived EVs identified by Anselmo et al. [21]. By combing the merits of lipid bilayer and peptide probes, our method may provide a valuable tool for the detection of cardiomyocyte-derived EVs in biological fluids, which may have a good application prospect in clinical diagnosis.

Materials and methods

Chemicals and materials

Peptide probes (Table S1) were synthesized by Sangon Biotech (Shanghai) Co., Ltd. (Shanghai, China). 1,2-Dipalmitoyl-sn-glycero-3-phosphocholine (DPPC), 1,2-dipalmitoyl-sn-glycero-3-phosphothioethanol (DPPTE), and *p*-sulfonatocalix[4]arene (pSC_4) were ordered from Macklin Inc. (Shanghai, China). Other chemicals, including silver nitrate and sodium borohydride, were purchased from Sinopharm Chemical Reagent Co., Ltd. (Shanghai, China). Heart myoblast cells H9C2 were purchased from Procell Life Science & Technology Co., Ltd. (Wuhan, China). Dulbecco's modified Eagle's medium (DMEM) (high glucose), fetal bovine serum (FBS), and antibiotic mixture were obtained from Thermo Fisher Scientific (Shanghai, China). Serum-free media and exosome-free FBS were purchased from Absin Bioscience Inc. (Shanghai, China). Hieff® Quick exosome isolation kit was purchased from Yeasen Biotechnology (Shanghai) Co., Ltd. (Shanghai, China).

Preparation of peptide-anchored biomimetic interface

Gold electrode (GE) was first cleaned and pretreated according to previous report [22]. Afterward, the electrode was used for the formation of a lipid bilayer using the paint-freeze method. In detail, 2 mM DPPTE (50 μL) was dipped on the surface of GE and reacted at room temperature for 16 h to generate the first layer of lipid through the Au–S interaction. Then, the electrode was rinsed with ethanol and further incubated with DPPC (20 mg mL^{-1}) for 5 min. After being kept at – 20 °C for 30 min and room temperature for 30 min in sequence, a lipid layer was successfully self-assembled on the GE surface. Peptide anchoring was then performed by immersing the electrode in 50 μL of 1 μM peptide probes for 1 h. Finally, the resulting peptide-anchored biomimetic interface was rinsed with PBS and kept at 4 °C for use.

Preparation of pSC_4-modified silver nanoparticles

pSC_4-modified silver nanoparticles (pSC_4-AgNPs) were prepared by referring to literature report [23]. In brief, 98 mL of 0.204 mM silver nitrate and 2 mL of 10 mM pSC_4 were mixed together and incubated for 20 min under vigorous stirring. Subsequently, a freshly prepared solution of 5 mM sodium borohydride was added to the mixture, followed by an additional stirring for 10 min. After that, the mixture was kept in the dark overnight and then centrifuged at 10,000 rpm for 10 min. The resulting precipitates as pSC_4-AgNPs were re-dispersed in double-distilled water and placed at 4 °C for further use.

Cell culture and isolation of EVs

Cardiomyocyte-derived EVs were isolated from the culture medium of H9C2 cells. In detail, H9C2 cells were cultured in DMEM (high glucose) with the addition of 10% FBS and 1% antibiotic mixture at 37 °C. Once the cells were grown to 70–80% confluence, they were separated and transferred to be grown in serum-free media for another 24–48 h. After that, the culture medium was collected and centrifuged at 3000 g for 10 min. The supernatant was then used for the isolation of EVs using Hieff® Quick exosome isolation kit under the manufacturer's instruction. The isolated EVs were dispersed in PBS and stored at – 80 °C before use.

Electrochemical detection of cardiomyocyte-derived EVs

Electrochemical detection of cardiomyocyte-derived EVs was performed by firstly dipping 20 μL of sample solutions that contained desired concentrations of H9C2 cells-derived EVs onto the peptide-anchored biomimetic interface, so as to achieve the enrichment of target EVs. After an incubation at room temperature for 1 h, the electrode was thoroughly washed with PBS and reacted with 100 μL of pSC_4-AgNPs. The reaction was held at room temperature for 45 min. After that, the electrode was washed again with PBS and applied in electrochemical measurements. All electrochemical measurements including electrochemical impedance spectrum (EIS) and linear sweep voltammetry (LSV) were carried out using a CHI660D workstation (Shanghai, China). EIS

measurements were performed in 5 mM $[Fe(CN)_6]^{3-/4-}$ with the parameters as follows: bias potential, 0.224 V; amplitude, 5 mV; and frequency range, 0.1 Hz to 10 kHz. LSV measurements were performed in 1 M KCl over the potential range of − 0.08 to 0.12 V.

Results and discussion

Principle of the electrochemical method for cardiomyocyte-derived EVs detection

Scheme 1 may illustrate the principle of the electrohemical method for detecting cardiomyocyte-derived EVs. Specifically, a peptide-anchored biomimetic interface is first fabricated at the surface of GE to provide desirable environments for recognizing and binding to target EVs. On the one hand, a lipid bilayer is self-assembled on the electrode surface and generates a hydration layer that significantly resists the nonspecific adsorption of proteins and other biological components. On the other hand, peptide probes are anchored into the lipid bilayer with the help of palmitoyl groups labelled at N-terminus, and show a specific affinity for CD172a because they contain the sequence of the "Self" peptide [13]. When cardiomyocyte-derived EVs are presented, the EVs are enriched onto the biomimetic interface via the interaction of peptide probes and CD172a expressed on the EVs. After that, pSC_4-AgNPs are recruited onto the surface of enriched EVs as signaling nanoprobes, which finally generate obvious electrochemical responses for the detection of target cardiomyocyte-derived EVs.

Characterization of peptide-anchored biomimetic interface

Peptide-anchored biomimetic interface is the critical element of the method, so we first carried out a series of characterization experiments. Figure 1a shows the EIS results for the step-by-step characterization of the biomimetic interface. The impedance spectrum of bare GE was nearly a straight line, suggesting that the electron transfer of electroactive $Fe[(CN)_6]^{3-/4-}$ was almost unrestricted (curve a). Once a lipid bilayer was self-assembled on the electrode surface, an obvious semicircle was obtained in the Nyquist spectrum (curve b), indicating the increase of electron transfer resistance. When the electrode was further incubated with peptide probes, an increase in the semicircle diameter was observed (curve c). This indicated that peptide probes were anchored onto the electrode surface by the interaction of N-terminal-labelled palmitoyl groups and the lipid bilayer, resulting in greater steric effect and enhanced blocking of electron transfer. The EIS results were in line with our expectations and

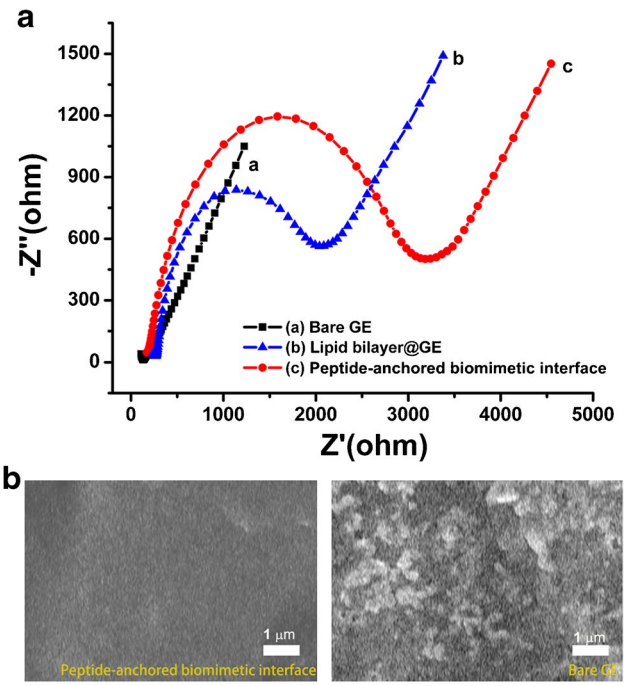

Fig. 1 **a** EIS results of (a) the bare GE, (b) the lipid bilayer-coated GE (lipid bilayer@GE), and (c) the peptide-anchored biomimetic interface. Three independent experimental repeats were performed for the EIS measurements. **b** SEM images of peptide-anchored biomimetic interface (left) and bare GE (right) after treatment of FBS. Scale bars, 1 μm

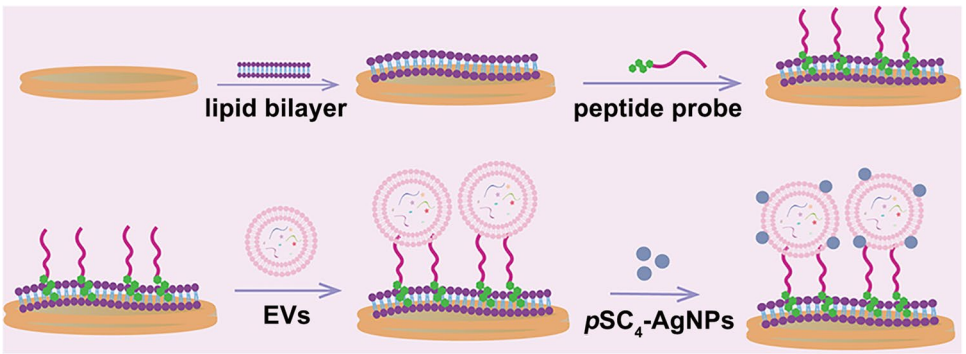

Scheme 1 Schematic illustration of electrochemical detection of cardiomyocyte-derived EVs detection based on peptide-anchored biomimetic interface

confirmed the successful fabrication of peptide-anchored biomimetic interface. After that, scanning electron microscopy (SEM) was employed to investigate the resistance of the biomimetic interfaces to non-specific adsorption. To do so, the peptide-anchored biomimetic interface and the bare GE were exposed to FBS for 2 h, respectively. As shown in Fig. 1b, after FBS treatment and thoroughly washing, the peptide-anchored biomimetic interface remained basically smooth, whereas the surface of bare GE became significantly rougher. The comparison clearly revealed that the biomimetic interface possessed superior antifouling ability and could act as a barrier against non-specific adsorption of proteins and other components in biological fluids (e.g., serum).

Feasibility of peptide-anchored biomimetic interface for the detection of cardiomyocyte-derived EVs

Having verified the formation of peptide-anchored biomimetic interface, we proceeded to investigate whether the interface could be used to detect cardiomyocyte-derived EVs. For proof-of-principle studies, EVs that were isolated from H9C2 cells were used as model cardiomyocyte-derived EVs. Transmission electron microscope (TEM) image revealed the typical bilayer membrane structure of the EVs (Fig. S1). Nanoparticle tracking analysis showed a wide size distribution of the EVs, ranging from 50 to 500 nm (Fig. S2). Flow cytometry analysis proved the positive expression of CD172a at the EVs by using anti-CD172a-functionalized immune magnetic beads (anti-CD172a@IMBs) and Dio staining (Fig. 2a). EIS was utilized to verify the enrichment of target EVs to the peptide-anchored biomimetic interface. As shown in Fig. 2b, the incubation of H9C2 cells-derived EVs caused an obvious increase in the semicircle diameter (curve b versus curve a). However, once the peptide probes were replaced by control peptide probes (cPep) that did not contain the sequence of "Self" peptide, the H9C2 cells-derived EVs treatment induced nearly no change in the Nyquist spectra (curve c and curve d). These EIS results demonstrated that cardiomyocyte-derived EVs could be enriched to the peptide-anchored biomimetic interface and that the enrichment depended on the specific interaction between the peptide probes and CD172a on the EVs surface.

After the enrichment of target EVs, pSC$_4$-AgNPs were employed as signaling nanoprobes in view of their universal binding to amino acid residues and their solid-state Ag/AgCl voltammetry response [23]. Figure S3 displays the TEM image of pSC$_4$-AgNPs, showing uniform particle distribution. Figure S4 displays the typical LSV response of pSC$_4$-AgNPs with a sharp and significant peak, consistent with the previous report [23]. Figure 3a shows the LSV response for the detection of 1×10^8 particles/mL H9C2 cells-derived EVs by the combined use of peptide-anchored biomimetic interface and pSC$_4$-AgNPs, and those obtained in control experiments. Obviously, the LSV peak for H9C2 cells-derived EVs (curve a) was much higher than that obtained in the absence of the EVs (curve b), which proved that the method was feasible for the detection of cardiomyocyte-derived EVs. Additionally, a control experiment was performed in the presence of 1×10^8 particles/mL target EVs but using bare AgNPs instead of pSC$_4$-AgNPs. As shown in curve c, a quite low LSV peak was observed in this case. This indicated that bare AgNPs could not bind directly to the enriched EVs surface, revealing that the recruitment of pSC$_4$-AgNPs was dependent on the recognition between pSC$_4$ and amino acid residues on EVs surface. Control experiments were also carried out to detect EVs derived from other cell sources, including the breast epithelial cell MCF-10A and the liver cell L-02. Flow cytometry analysis revealed the negative expression of CD172a at the EVs derived from either MCF-10A or L-02 cells (Fig. S5). Similar results were observed in the electrochemical detection. As shown in Fig. 3b, the peak currents obtained for detecting 1×10^8 particles/mL

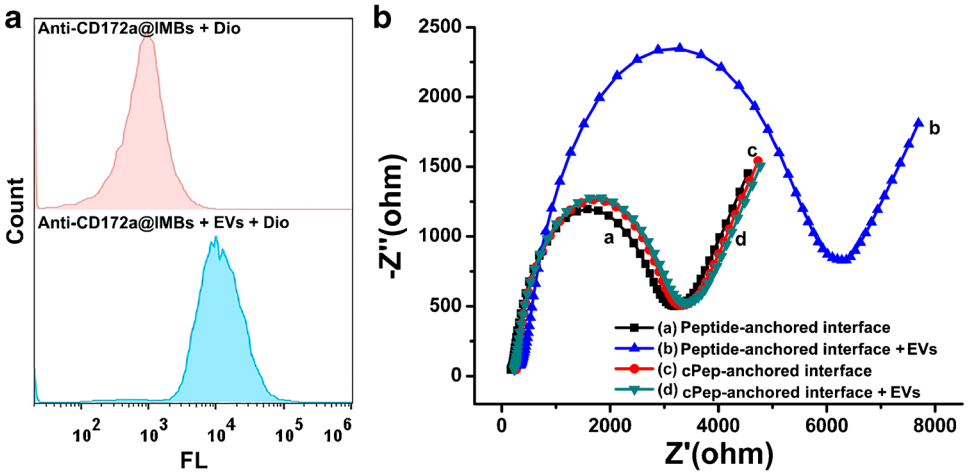

Fig. 2 **a** Flow cytometry analysis of H9C2 cells-derived EVs captured by anti-CD172a@IMBs after Dio staining. **b** EIS results of the peptide-anchored biomimetic interface (a) before and (b) after incubated with H9C2 cells-derived EVs. Curves c and d correspond to the EIS results of the cPep-anchored biomimetic interface before and after incubated with H9C2 cells-derived EVs

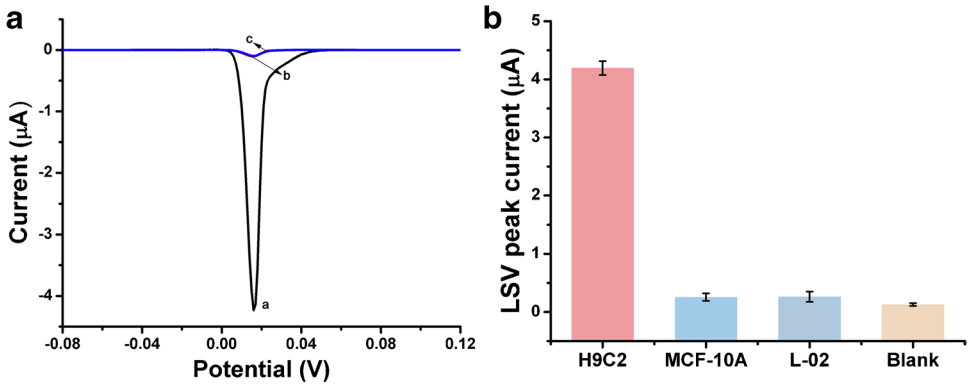

Fig. 3 **a** LSV responses for detecting (a) 1×10^8 particles/mL or (b) 0 particles/mL H9C2 cells-derived EVs. Curve c corresponds to the LSV response for detecting 1×10^8 particles/mL H9C2 cells-derived EVs using bare AgNPs. **b** LSV peak currents for detecting 1×10^8 particles/mL EVs derived from H9C2, MCF-10A, and L-02 cells. The blank corresponds to the group without EVs

MCF-10A and L-02 cells-derived EVs approximated that for the blank group, but were much lower than that for 1×10^8 particles/mL H9C2 cells-derived EVs, which demonstrated the high specificity of the method.

Electrochemical detection of cardiomyocyte-derived EVs

Encouraged by its feasibility, the method was then applied to detect different concentrations of cardiomyocyte-derived EVs. To achieve the best detection performance, the reaction time for target EVs enrichment was optimized. As shown in Fig. S6, the LSV peak current increased with the elongation of the reaction time until 60 min. So, 60 min was chosen as the optimal enrichment time. The reaction time for pSC$_4$-AgNPs incubation was also optimized, which suggested an optimal time of 45 min (Fig. S7). Figure 4a shows the results for the quantitative analysis of H9C2 cells-derived EVs under the optimized conditions, revealing that the LSV responses increased with increasing concentrations of target EVs. This is reasonable because more H9C2 cells-derived EVs enriched onto the peptide-anchored biomimetic interface subsequently recruited enhanced amounts of pSC$_4$-AgNPs to generate larger LSV response. Figure 4b further shows the relationship between the LSV peak current and the concentration of H9C2 cells-derived EVs. It can be seen that the LSV peak current (I) aggrandized in a concentration-dependent manner and exhibited a good linear correlation with the logarithmic value of target EV concentration (C_{EV}) ranging from 1×10^3 to 1×10^8 particles/mL. The linear equation was I (μA) = $0.667\times\mathrm{Log}C_{EV}$ (particles/mL) − 1.256, $R^2 = 0.997$. The detection limit was calculated to be 132 particles/mL at a signal-to-noise ratio of 3, which was comparable or even better than that of existing electrochemical methods for EVs detection (Table S2) [24–29].

The usability of the method in complex environment was also investigated. To do this, H9C2 cells-derived EVs were diluted in PBS and exosome-free FBS to three different concentrations (1×10^4, 1×10^5, and 1×10^6 particles/mL) and detected using our method. As shown in Fig. S8, LSV peak currents for the EVs with the same concentration in the two kinds of samples were basically the same, showing no significant difference between each other. Moreover, the method was applied to directly detect cardiomyocyte-derived EVs

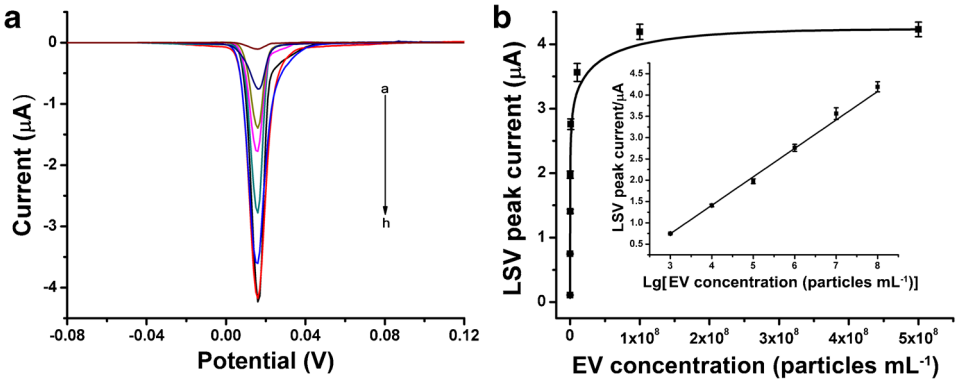

Fig. 4 **a** LSV responses obtained with different concentrations of H9C2 cells-derived EVs (from a to h: 0, 1×10^3, 1×10^4, 1×10^5, 1×10^6, 1×10^7, 1×10^8, 5×10^8 particles/mL). **b** Calibration curve for the electrochemical detection of H9C2 cells-derived EVs. Inset shows the linear relationship between the LSV peak current and the logarithmic value of the EV concentration ranging from 1×10^3 to 1×10^8 particles/mL. Error bars represent the standard deviations of the three independent measurements

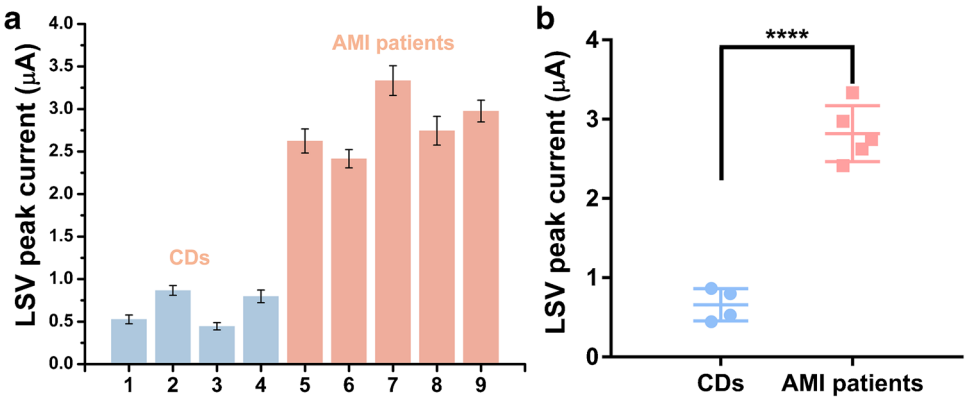

Fig. 5 **a** LSV peak currents for detecting cardiomyocyte-derived EVs in serum samples from CDs and AMI patients. **b** Scatter plots of the LSV peak currents in **a**. Statistical significance was calculated by two-tailed Student's *t* test; ****$p < 0.0001$

in serum samples collected from acute myocardial infarction (AMI) patients ($n = 5$) and control donors (CDs, $n = 4$) with informed consent. The clinical experiment was approved by the Ethics Committee of People's Hospital of Leshan and performed according to ethical standards. As shown in Fig. 5, LSV peak currents obtained in the AMI patient samples were much higher than those obtained in the CD samples. The average values of LSV peak currents for AMI patients and CDs were 2.82 μA and 0.66 μA, respectively, showing a significant statistical difference. The results were in good agreement with previous report [21], demonstrating that the method had a good applicability in complex environment and a potential use in clinical diagnosis, which would be attributed to the good antifouling ability of the biomimetic interface.

Conclusions

In conclusion, we have fabricated a peptide-anchored biomimetic interface and successfully used it for the electrochemical detection of cardiomyocyte-derived EVs. The use of lipid layer provided convenience for the anchoring of CD172a-targeting peptides and effectively reduced the non-specific adsorption of proteins and other components in biological fluids in view of good antifouling property, which ensured the clinical applicability of the detection method. Meanwhile, the use of pSC_4-AgNPs with extensive binding to surface proteins guaranteed the recruitment efficiency of the nanoprobes, and their excellent solid-state Ag/AgCl voltammetry responses laid the foundation for the sensitive detection of target EVs. Experimental results showed that the method could be used to detect target EVs with a detection limit of 132 particles/mL, which was lower or comparable to existing electrochemical methods, and exhibited desirable performance in serum samples. Therefore, the method may provide a valuable tool for cardiomyocyte-derived EVs detection and have a good application prospect in the diagnosis of cardiac diseases.

Supplementary information The online version contains supplementary material available at https://doi.org/10.1007/s00216-022-04419-3.

Author contribution All authors contributed to the study conception and design. The first draft of the manuscript was written by YZ, and all authors commented on previous versions of the manuscript. All authors read and approved the final manuscript.

Funding This work was supported by the grant from Sichuan Medical Association (No. Q17041).

Data availability All data generated or analyzed during this study are included in this article and its supplementary information file.

Declarations

Ethics approval Clinical experiment was approved by the Ethics Committee of People's Hospital of Leshan and performed according to ethical standards.

Competing interests The authors declare no competing interests.

Source of biological material Serum samples were collected from AMI patients and control donors with informed consent.

References

1. Ouyang M, Tub D, Tong L, Sarwar M, Bhimaraj A, Li C, Coté GL, Di Carlo D. A review of biosensor technologies for blood biomarkers toward monitoring cardiovascular diseases at the point-of-care. Biosens Bioelectron. 2021;171:112621. https://doi.org/10.1016/j.bios.2020.112621.
2. Davidson SM, Boulanger CM, Aikawa E, Badimon L, Barile L, Binder CJ, Brisson A, Buzas E, Emanueli C, Jansen F, Katsur M, Lacroix R, Lim SK, Mackman N, Mayr M, Menasché P, Nieuwland R, Sahoo S, Takov K, Thum T, Vader P, Wauben MHM, Witwer K, Sluijter JPG. Methods for the identification and characterization of extracellular vesicles in cardiovascular studies: from exosomes to microvesicles. Cardiovasc Res. 2022. https://doi.org/10.1093/cvr/cvac031.

3. Fu S, Zhang Y, Li Y, Luo L, Zhao Y, Yao Y. Extracellular vesicles in cardiovascular diseases. Cell Death Discov. 2020;6:68. https://doi.org/10.1038/s41420-020-00305-y.
4. Zarà M, Amadio P, Campodonico J, Sandrini L, Barbieri SS. Exosomes in cardiovascular diseases Diagnostics. 2020;10:943. https://doi.org/10.3390/diagnostics10110943.
5. Sahoo S, Adamiak M, Mathiyalagan P, Kenneweg F, Kafert-Kasting S, Thum T. Therapeutic and diagnostic translation of extracellular vesicles in cardiovascular diseases: roadmap to the clinic. Circulation. 2021;143:1426–49. https://doi.org/10.1161/CIRCULATIONAHA.120.049254.
6. Zamani P, Fereydouni N, Butler AE, Navashenaq JG, Sahebkar A. The therapeutic and diagnostic role of exosomes in cardiovascular diseases. Trend Cardiovas Med. 2019;29:313–23. https://doi.org/10.1016/j.tcm.2018.10.010.
7. Min L, Wang B, Bao H, Li X, Zhao L, Meng J, Wang S. Advanced nanotechnologies for extracellular vesicle-based liquid biopsy. Adv Sci. 2021;8:2102789. https://doi.org/10.1002/advs.202102789.
8. Singh S, Numan A, Cinti S. Electrochemical nanobiosensors for the detection of extracellular vesicles exosomes: from the benchtop to everywhere? Biosens Bioelectron. 2022;216:114635. https://doi.org/10.1016/j.bios.2022.114635.
9. Feng Q, Fan W, Ren W, Liu C. Recent advances in exosome analysis assisted by functional nucleic acid-based signal amplification technologies. TrAC Trend Anal Chem. 2022;149:116549. https://doi.org/10.1016/j.trac.2022.116549.
10. Shao H, Im H, Castro CM, Breakefield X, Weissleder R, Lee H. New technologies for analysis of extracellular vesicles. Chem Rev. 2018;118:1917–50. https://doi.org/10.1021/acs.chemrev.7b00534.
11. Kaya SI, Ozcelikay G, Mollarasouli F, Bakirhan NK, Ozkan SA. Recent achievements and challenges on nanomaterial based electrochemical biosensors for the detection of colon and lung cancer biomarkers. Sens Actuator B-Chem. 2022;351:130856. https://doi.org/10.1016/j.snb.2021.130856.
12. Bakirhan NK, Topal BD, Ozcelikay G, Karadurmus L, Ozkan SA. Current advances in electrochemical biosensors and nanobiosensors. Crit Rev Anal Chem. 2022;52:519–34. https://doi.org/10.1080/10408347.2020.1809339.
13. Rodriguez PL, Harada T, Christian DA, Pantano DA, Tsai RK, Discher DE. Minimal "Self" peptides that inhibit phagocytic clearance and enhance delivery of nanoparticles. Science. 2013;339:971–5. https://doi.org/10.1126/science.12295.
14. Li C, Huang Y, Yang Y. Coupling of an antifouling and reusable nanoplatform with catalytic hairpin assembly for highly sensitive detection of nucleic acids using zeta potential as signal readout. Sens Actuator B-Chem. 2021;326:128845. https://doi.org/10.1016/j.snb.2020.128845.
15. Li H, Dauphin-Ducharme P, Arroyo-Curras N, Tran CH, Vieira PA, Li SG, Shin C, Somerson J, Kippin TE, Plaxco KW. A biomimetic phosphatidylcholine-terminated monolayer greatly improves the in vivo performance of electrochemical aptamer-based sensors. Angew Chem Int Ed. 2017;56:7492–5. https://doi.org/10.1002/anie.201700748.
16. McKeating KS, Hinman SS, Rais NA, Zhou ZG, Cheng Q. Antifouling lipid membranes over protein A for orientation-controlled immunosensing in undiluted serum and plasma. ACS Sens. 2019;4:1774–82. https://doi.org/10.1021/acssensors.9b00257.
17. Dong G, An Y, Yan P, Wu J, Li C, Liu T. A zeta potential-based homogeneous assay for amplified detection of telomerase in cancer cells. Sens Actuator B-Chem. 2022;350:130881. https://doi.org/10.1016/j.snb.2021.130881.
18. Manna SL, Di Natale C, Onesto V, Marasco D. Self-assembling peptides: from design to biomedical applications. Int J Mol Sci. 2021;22:12662. https://doi.org/10.3390/ijms222312662.
19. Loew M, Springer R, Scolari S, Altenbrunn F, Seitz O, Liebscher J, Huster D, Herrmann A, Arbuzova A. Lipid domain specific recruitment of lipophilic nucleic acids: a key for switchable functionalization of membranes. J Am Chem Soc. 2010;132:16066–72. https://doi.org/10.1021/ja105714r.
20. Zhang P, Cui Y, Anderson CF, Zhang C, Li Y, Wang R, Cui H. Peptide-based nanoprobes for molecular imaging and disease diagnostics. Chem Soc Rev. 2018;47:3490–529. https://doi.org/10.1039/C7CS00793K.
21. Anselmo A, Frank D, Papa L, Anselmi CV, Di Pasquale E, Mazzola M, Panico C, Clemente F, Soldani C, Pagiatakis C, Hinkel R, Thalmann R, Kozlik-Feldmann R, Miragoli M, Carullo P, Vacchiano M, Chaves-Sanjuan A, Santo N, Losi MA, Ferrari MC, Puca AA, Christiansen V, Seoudy H, Freitag-Wolf S, Frey N, Dempfle A, Mercola M, Esposito G, Briguori C, Kupatt C, Condorelli G. Myocardial hypoxic stress mediates functional cardiac extracellular vesicle release. Eur Heart J. 2021;42:2780–92. https://doi.org/10.1093/eurheartj/ehab247.
22. Tang Y, Dai Y, Huang X, Li L, Han B, Cao Y, Zhao J. Self-assembling peptide-based multifunctional nanofibers for electrochemical identification of breast cancer stem-like cells. Anal Chem. 2019;91:7531–7. https://doi.org/10.1021/acs.analchem.8b05359.
23. Zhang J, Chen H, Cao Y, Feng C, Zhu X, Li G. Design nanoprobe based on its binding with amino acid residues on cell surface and its application to electrochemical analysis of cells. Anal Chem. 2019;91:1005–10. https://doi.org/10.1021/acs.analchem.8b04247.
24. Sha L, Bo B, Yang F, Li J, Cao Y, Zhao J. Programmable DNA-fueled electrochemical analysis of lung cancer exosomes. Anal Chem. 2022;94:8748–55. https://doi.org/10.1021/acs.analchem.2c01318.
25. Cao Y, Wang Y, Yu X, Jiang X, Li G, Zhao J. Identification of programmed death ligand-1 positive exosomes in breast cancer based on DNA amplification-responsive metal-organic frameworks. Biosens Bioelectron. 2020;166:112452. https://doi.org/10.1016/j.bios.2020.112452.
26. Miao P, Ma X, Xie L, Tang Y, Sun X, Wen Z, Wang Z. Tetrahedral DNA mediated direct quantification of exosomes by contact-electrification effect. Nano Energy. 2022;92:106781. https://doi.org/10.1016/j.nanoen.2021.106781.
27. Zhang H, Qiao B, Guo Q, Jiang J, Cai C, Shen J. A facile and label-free electrochemical aptasensor for tumour-derived extracellular vesicle detection based on the target-induced proximity hybridization of split aptamers. Analyst. 2020;145:3557–63. https://doi.org/10.1039/D0AN00066C.
28. Sabaté del Río J, Woo HK, Park J, Ha HK, Kim JR, Cho YK. SEEDING to enable sensitive electrochemical detection of biomarkers in undiluted biological samples. Adv Mater. 2022;34:2200981. https://doi.org/10.1002/adma.202200981.
29. Lee M, Park SJ, Kim G, Park C, Lee MH, Ahn JH, Lee T. A pretreatment-free electrical capacitance biosensor for exosome detection in undiluted serum. Biosens Bioelectron. 2022;199:113872. https://doi.org/10.1016/j.bios.2021.113872.